Research paper

Structure, CO-releasing property, electrochemistry, DFT calculation, and antioxidant activity of benzimidazole derivative substituted $[Mn(CO)_3(bpy)L]PF_6$ type novel manganese complexes

Elvan Üstün, Melek Çol Ayvaz, Mutlu Sönmez Çelebi, Gizem Aşci, Serpil Demir, İsmail Özdemir

PII: S0020-1693(16)30269-9
DOI: http://dx.doi.org/10.1016/j.ica.2016.05.027
Reference: ICA 17063

To appear in: *Inorganica Chimica Acta*

Received Date: 25 February 2016
Revised Date: 10 May 2016
Accepted Date: 12 May 2016

Please cite this article as: E. Üstün, M.C. Ayvaz, M.S. Çelebi, G. Aşci, S. Demir, I. Özdemir, Structure, CO-releasing property, electrochemistry, DFT calculation, and antioxidant activity of benzimidazole derivative substituted $[Mn(CO)_3(bpy)L]PF_6$ type novel manganese complexes, *Inorganica Chimica Acta* (2016), doi: http://dx.doi.org/10.1016/j.ica.2016.05.027

Structure, CO-releasing property, electrochemistry, DFT calculation, and antioxidant activity of benzimidazole derivative substituted $[Mn(CO)_3(bpy)L]PF_6$ type novel manganese complexes

Elvan ÜSTÜN[a], Melek ÇOL AYVAZ[a*], Mutlu SÖNMEZ ÇELEBİ[a], Gizem AŞCI[a], Serpil DEMİR[b], İsmail ÖZDEMİR[b],

[a] Department of Chemistry, Faculty of Science and Arts, Ordu University, 52200, Ordu, Turkey

[b] Department of Chemistry, Faculty of Science, İnönü University, 44280, Malatya, Turkey

Corresponding Author: mcol@odu.edu.tr

ABSTRACT

Metal carbonyl complexes are prominent group organometallic compounds because of their applications in industrial and pharmaceutical chemistry. In recent years, metal carbonyl complexes have been accepted major for storage and transportation of carbon monoxide which is an important signaling molecule significantly in pathogenesis of some diseases. Thus, we designed and synthesized novel manganese(I)carbonyl complexes with general formula $[Mn(CO)_3(bpy)L]PF_6$ (bpy=2,2-bipyridyl, L= N-(2-chlorobenzyl)benzimidazole, N-(2-methoxybenzyl)benzimidazole, N-(2-methylbenzyl)benzimidazole). The complex molecules were characterized by LC-MS, ^{1}H-NMR, ^{13}C-NMR, IR spectroscopy methods and elemental analysis. The CO-releasing properties, antioxidant activities and redox properties of these complexes were investigated. The DFT/TDDFT analyses were made by ORCA package program.

INTRODUCTION

Since the discovery of nickel tetracarbonyl more than a century ago [1], metal carbonyls have played a very important role in pharmaceutical chemistry. These complexes are now established as useful biomolecules. The work on CO intensified, metal carbonyl complexes which have been accepted major for storing and transporting CO are antiinflammatory, antiapoptotic, and antiproliferative, protects tissues against hypoxia or ischemia-reperfusion injury, and causes vasodilatation [2]. The studies show that endogenous increase of the CO amount in a tissue plays a role in eliminating the problem and regulating the intracellular functions [3-8]. It has been also shown to have an appreciable

role in preclinical animal models of cardiovascular disease, inflammatory disorders, and organ transplantation [9-13].

Reactive oxygen species (ROS) are highly reactive molecules and can damage cell structures such as carbohydrates, nucleic acids, lipids, and proteins and alter their functions. Antioxidant systems which include enzymatic and nonenzymatic antioxidants are usually effective in blocking harmful effects of ROS. The shift in the balance between oxidants and antioxidants in favor of oxidants is termed "oxidative stress" and changes in oxidative stress are associated with reciprocal changes in antioxidant capacity [14, 15]. Srisook et al. employed CORM-2 molecule to demonstrate that CO can inhibit ROS production, especially O_2^- and NO, with murine macrophage cell line RAW 264.7 [16]. Backer et al. studied with CORM-3 on surgical manipulated mice intestine about antioxidant effect of CO and revealed that treatment with CORM-3 partially reduced oxidative stress in the muscularis externa and confirmed a direct protective effect of CO in addition to the ability to induce HO-1 [17]. However, the inhibition of the early "oxidative burst" in the mucosa fully depended on the induction of HO-1. Similarly, Lamon et al. tried to enlighten with CORM-3 that CO acts whether as a vasodilator or vasoconstrictor on vascular endothelial cells depending on ROS [18]. Although there are discrepancies about the mechanism of action, it is apparent that CO and CORMs are really worth checking out in point of antioxidant activity and an in-vitro molecular antioxidant activity study of novel CORM may provide significant contribution while being directive for possible therapeutic applications.

Benzimidazole derivatives have been proven to function as antihypertensive [19], antiinflammatory [20], antimicrobial [21], antiviral [22-24], antitumor [24-26], anticoagulants [27], antidiabetic [28] agents. Benzimidazole derivatives are also useful antioxidants [29]. Transition metal complexes with benzimidazoles can be tested in bioinorganic systems and may exhibit synergistic effect in possible therapeutic applications.

Safe transmission of appropriate amount of CO to the tissue is crucial, and one of the most promising candidates for this mission is metal carbonyl complexes. Many carbonyl complexes of transition metals have been found to be photoreactive under irradiation into their lowest charge-transfer (CT) absorption band, the observed primary reaction corresponding to a carbonyl loss [30-36]. One of various ways to ensure CO-release is to irradiate the complexes with UV-light with certain wavelength. These kinds of dark-stable, light-sensitive and potentially CO-releaser complexes are called as photoCORMs (photo-activatable CO-releasing molecules) and manganese carbonyl complexes are well-known photoCORMs [37-43].

Charge-transfer transitions {metal-to-ligand (MLCT), ligand-to-metal (LMCT)} of metal carbonyls can lead to redox reactions and also result in reducing the metal center and generating radicals [44-46]. Density functional theory (DFT) and time-dependent density functional theory (TDDFT) are potent and efficient tools for excited-state characterization and decomposition pathways of transition metal

complexes and often show how a broad absorption band can conceal beneath it several electronic transitions. These are also essential for development of new molecules with suitable characteristics for biological applications. Similar calculations have also been used to better explain the redox behavior observed for carbonyls i.e., the specific location of the oxidizing or reducing equivalents in metal carbonyls [47-50].

Studies about analyses of bioactivity of CO and synthesis of new CO-releasing molecules have received considerable attention after the favorable results about functions of CO in tissue. It is clear from the reference list that, although new CORMs having more advantageous half-life and more totally released CO have been synthesized, research about biological function of CO has been focused on initial CORMs (CORM-2, CORM-3 etc.) which could be synthesized easily or obtained commercially [14]. We managed to give results in diverse fields for our novel molecules to provide guidance and convenience for further research. In this study, novel $[Mn(CO)_3(bpy)L]PF_6$ [bpy=2,2-bipyridyl, L= N-(2-chlorobenzyl)benzimidazole, N-(2-methoxybenzyl)benzimidazole, N-(2-methylbenzyl)benzimidazole] type manganese complexes with benzimidazole derivative ligands have been synthesized. The structures of the compounds were enlightened by ^{1}H-NMR, ^{13}C-NMR, IR, LC-MS, and elemental analysis. Basic level in-vitro molecular antioxidant activity, redox properties and CO-releasing properties have also been described hereunder. The excited-state characterization was rationalized by DFT/TDDFT with ORCA package program [51-54].

DISCUSSION

Novel $[Mn(CO)_3(bpy)L]PF_6$ [bpy=2,2-bipyridyl, L= N-(2-chlorobenzyl)benzimidazole, N-(2-methoxybenzyl)benzimidazole, N-(2-methylbenzyl)benzimidazole] type manganese complexes with benzimidazole derivative ligands have been synthesized (Figure 1).The characterization of the ligands and $Mn(CO)_3(bpy)Br$ were made by ^{1}H-NMR, ^{13}C-NMR and elemental analysis. The complexes 5-7 were characterized by ^{1}H-NMR, ^{13}C-NMR, IR and LC-MS and all characterization details could be analyzed in Results. One broad band (379 nm for **5**, 378 nm for **6**, and 380 nm for **7**) and a shoulder at 320 nm were observed for complexes 5-7 with lower intensity in UV-Vis Spectra. The absorbance maximas and molar extinction coefficients of complexes 5-7 were determined in dimethyl sulfoxide (Table 1).

Figure 1

CO-releasing properties of the complexes were identified by myoglobin-assay as detailed below. Since the complexes are light sensitive but dark stable (photoCORMs), 366 nm UV lamp was used for releasing (Figure S1 and Figure S2). Total released CO, CO equivalents, the percentage released CO and half-life ($t_{1/2}$) were determined with UV-Visible Spectrophotometer at 1 minute intervals (Figure

2). The $t_{1/2}$ in this study is defined as the time taken for compounds 5-7 to release 50% of the total CO ligands present per molecule.

Figure 2

In myoglobin assay, due to binding of released CO with myoglobin, the reaction is forced towards product side. Carbonmonoxymyoglobin concentration [MbCO] and equivalence CO (eq. CO) which become fixed after a while have been indicated total released CO. Molecule **5**, the most efficient in this study, released 2.19 of 3 carbon monoxide when 32.84 µM of carbonmonoxymyoglobin was formed. Carbonmonoxymyoglobin concentration of **6** was 27.73 µM while the equivalence CO was 1.85. The amount of CO released as well as the release rate is obviously dependent on the nature of the substituents on benzyl, the rest of the molecules are identical. Although it is not possible to have common decision with three molecules, the results can be associated with mesomeric and inductive effect of the substituents. Methoxy, more effective mesomeric substituent than chlorine and methyl, induces the increasing of electron density on metal center and metal-CO back-bonding. Strong back-bonding means difficult releasing of CO. On the other hand, chlorine has both inductive and mesomeric effect while methyl has only inductive effect which is more dominant than the mesomeric effect for chlorine. Half-lives of the molecules can be used for kinetic analysis. Most advantageous molecule according to half-life is **7** which released half of its CO in 7.31 minute while the slowest one is **6** with 11.07 minute. It is possible to pay attention that the more efficient CO-releaser is the slowest one (Table 1).

Table 1

The released CO amount has been determined by myoglobin assay and also followed IR spectra. Provided that the CO releasing occurs as observed in the myoglobin assay, the reactions would result with the formation of di- or monocarbonyl complexes of manganese. Typical IR spectra for manganese (I) fac-tricarbonyl complexes with a strong band 2030 cm^{-1} and two additional bands around 1925 cm^{-1} were observed before illumination (Figure S3). During excitations, strong IR bands of initial complexes disappeared indicating the dissociation of $[Mn^{I}(CO)_3]$-units of complexes. On the other hand new IR bands emerged in the region around 1975 cm^{-1} and 1860 cm^{-1}. These bands could be the indication of manganese (I) cis-dicarbonyl complexes [55, 56]. Ultimate IR bands which took shape on 5th minute around 1850 cm^{-1} and 1875 cm^{-1} might be the sign for monocarbonyl manganese (I) complexes [57].

Many transition metal complexes exhibit antioxidant activity [58]. Therefore, an *in vitro* investigation was carried out to explore whether the compounds 5-7 have 2,2-diphenyl-1-picrylhydrazyl (DPPH), superoxide (O_2^{-}) and nitroxyl (NO·) radical scavenging activities.

As can be seen from the Table 2, DPPH scavenging ratios (%) of the 0.2 mM of all investigated compounds were under 10% without UV exposure. But at the end of UV light exposure for 10 minutes, observed scavenging ratios were increased for each. Moreover, for compound **7**, it is seen that this increment continues at the end of the exposure time for 20 min. Even in this case, the highest calculated inhibition percentage is lower than the calculated value for ascorbic acid (AA), which is used as a standard antioxidant. 0.2 mM AA scavenged the 89.8 % of the DPPH radicals in the medium under the same conditions.

Unlike DPPH radical scavenging activities, superoxide radical scavenging activities of the compounds 5-7 increased due to CO releasing and reached a high value comparable with the value calculated using commercial SOD enzyme.

Table 2

Among these assays, the most interesting results were obtained for NO· radical scavenging abilities in which CO releasing led to a decline in activity. Nitroxyl radical scavenging activities of these CORMs were also higher than found for AA under the same conditions. The results are consistent with findings in the literature recorded by Choi et al., 2015 [59]. They had proved that the CO-releasing molecule-3 suppressed *Prevotella* inter-media lipopolysaccharide-induced production of nitric oxide.

The results obtained by three different methods confirmed that the investigated compounds are more effective to arrest superoxide radicals than the other radicals.

Figure 3

The electrochemical behaviors of the complexes were investigated by cyclic voltammetry on a stationary glassy carbon electrode in the potential range 2.0 V to -2.0 V vs. Ag/AgCl. CVs of the complexes are given in Figure 2 in acetonitrile containing 0.1 M TBAP at a scan rate of 50 mV s^{-1}. The nature of the voltammograms does not change with scan rate (50-200 mV s^{-1}). All three compounds show an irreversible oxidation peak around +1.4 V (1.40 V, 1.46 V and 1.48 V for compounds **5**, **6** and **7** respectively). As the potentials are quite close to each other, the peaks look almost unaffected by differentiating the ligands and therefore should be attributed to the metal center of the complexes rather than the ligand sites. These oxidation peaks are assigned to the monoelectronic oxidation of Mn(I) to Mn(II) [60]. A less intensive oxidation process around 0.0 V was also observed for all three compounds (-0.18 V, 0.27 V and 0.35 V for compounds **5**, **6** and **7** respectively) which is also irreversible. Unfortunately we have not been able to identify the species involved in the oxidation process. As seen from the voltammograms, all three compounds feature complicated oxidation and reduction peaks at the negative potential region. This behavior is assigned to ligand based oxidation/reduction of the complex molecules as the position of the peaks are

obviously affected by altering the substituents on the ligands coordinating the metal. The reduction process assigned to the ligand sites of the molecules may be referred to electron accommodation of the π^* MO of the ligand (the LUMO of the compound) which is clearly affected by the substituents (i.e. – Cl, – OCH_3, and – CH_3 for compounds **5**,**6** and **7** respectively). For example, when we compare the first reduction peaks of compounds **5** and **7** (-1.43 V and -1.76 V respectively), reduction of the latter is observed at a more negative potential. As the substituent becomes more electron withdrawing (as in the case of compound **5** relative to compound **7**), the relative energy of the π^* MO becomes lower which causes the compound to be reduced easier leading to a more positive reduction potential [61, 62]. As expected according to the electron withdrawing moieties of the substituents of the ligands, the first reduction peak of the compound **7** is observed at a more positive potential than compound **5**.

An understanding of the photochemistry of transition metal compounds requires knowledge of the properties of molecular orbitals and appropriate excited states. Frontier orbitals play a relevant role in such systems, because they rule the electronic excitations and the transition characters. With the aid of TDDFT calculations, it is possible to have comments about the contributions of the ligand and metal orbitals to molecular orbitals. It is not practical to analyze all the electronic transitions and the orbitals; therefore some restrictions were used. Only strong transitions with an oscillator strength >0.01 in the 300−600 nm range were reported and only contributions >10% were listed. The ground-state electronic structures were calculated accounting for the solvent effect of water in COSMO model.

For all complexes, the highest occupied molecular orbital (HOMO) is basically manganese-centered with limited contribution from benzimidazole and CO moieties like HOMO-1 and HOMO-2. In **5**, HOMO-4 and HOMO-6 are completely benzimidazole-based while HOMO-7 consists of bpy. The lowest unoccupied molecular orbital (LUMO) is localized on the bpy's for all complexes. LUMO+1 and the other unoccupied virtual orbitals, up to LUMO+3, are all ligand based but LUMO+5 and LUMO+6 have little manganese contributions. All molecular orbitals which have contribution to singlet electronic states can be seen in Table 3, Figure S3-S5, and Table S1-S3.

Table 3

One broad band (379 nm for **5**, 378 nm for **6** and 380 nm for **7**) and a shoulder at 320 nm were observed in the experimental spectra of complexes 5-7. These broad energy bands which calculated 377 nm for all molecules are attributed MLCT states (Mn → bpy; MLCT = metal-to-ligand charge transfer) with highest oscillator strength (f_{osc}) in TDDFT results. But the shoulders which occur 320 nm in experimental UV spectra for all complexes could not be confirmed with TDDFT calculations. The single calculated result at 321.2 nm with 0.0138 oscillator strength for **5** has contributions of HOMO-1→LUMO+5 (46.0%, MLCT Mn→imid), HOMO-1→LUMO+6 (37.6%, MLCT Mn→imid) and HOMO-6→LUMO+2 (10.2%, LLCT imid→bpy) transitions. Complex **6** and **7** haven't got a

suitable transition among calculated wavelength and oscillator strength in TDDFT results for 320 nm shoulder. Residual transitions of **5** which have contribution more than %10 but not given in Table S1 and all electronic transitions of **6** and **7** were given in Table S2 and Table S3. With the aid of DFT/TDDFT calculation, we had knowledge about frontier molecular orbitals, electronic transitions, and singlet excitation density differences of compounds.

RESULTS

N-(3-chlorobenzyl)benzimidazole (1)

Yield: 2.09 g (86.0%). ^{1}H NMR (300 MHz, $CDCl_3$): δ (ppm)= .26 (s, 1H, NC*H*N), 7.78-7.75 (m, 1H, NC_6H_4N), 7.48-7.37 (m, 2H, NC_6H_4N), 7.26-7.00 (m, 4H, $CH_2C_6H_4$(Cl)-3), 6.99-6.98 (m, 1H, NC_6H_4N), 5.87 (s, 2H, $CH_2C_6H_4$(Cl)-3). ^{13}C NMR (300 MHz, $CDCl_3$): δ (ppm) =141.9 (N*C*HN), 136.4, 133.6, 122.7, 121.9, 112.7, and 109.2 (NC_6H_4N), 129.7, 127.6, 127.1, 126.2, 125.5, and 124.1 ($CH_2C_6H_4$(Cl)-3), 49.9 ($CH_2C_6H_4$(Cl)-3), Anal. Calc. for $C_{14}H_{11}N_2Cl$ (242.70): C, 69.28; H, 4.57; N, 11.54. Found: C, 69.25; H, 4.61; N, 11.50%.

N-(3-methoxybenzyl)benzimidazole (2)

Yield: 3.12 g (87.2%). ^{1}H NMR (300 MHz, $CDCl_3$): δ (ppm)= 8.04 (s, 1H, NC*H*N), 7.87-7.84 (m, 1H, NC_6H_4N), 7.35-7.25 (m, 4H, NC_6H_4N and $CH_2C_6H_4(OCH_3)$-3), 6.88-6.74 (m, 3H, $CH_2C_6H_4(OCH_3)$-3), 5.35 (s, 2H, $CH_2C_6H_4(OCH_3)$-3), 3.76 (s, 3H, $CH_2C_6H_4(OCH_3)$-3). ^{13}C NMR (300 MHz, $CDCl_3$): δ (ppm) =143.5 (N*C*HN), 160.1, 143.1, 136.9, 133.9, 130.2, 123.2, 122.4, 120.3, 119.4, 113.4, 113.0 and 110.1(NC_6H_4N and $CH_2C_6H_4(OCH_3)$-3), 55.3 ($CH_2C_6H_4(OCH_3)$-3), 48.7 ($CH_2C_6H_4(OCH_3)$-3). Calc. for $C_{15}H_{14}N_2O$ (238.3): C, 75.61; H, 5.92; N, 11.76. Found: C, 75.59; H, 5.93; N, 11.73%.

N-(3-methylbenzyl)benzimidazole (3)

Yield: 5.82 g (95.4%). ^{1}H NMR (300 MHz, $CDCl_3$): δ (ppm)= 2.33 (s, 3H, $NCH_2C_6H_4(CH_3)$-3), 5.33 (s, 2H, $NCH_2C_6H_4(CH_3)$-3), 7.00-7.86 (m, 8H, NC_6H_4N, $NCH_2C_6H_4(CH_3)$-3), 7.98 (s, 1H, NC*H*N). ^{13}C NMR (300 MHz, $CDCl_3$): δ (ppm) =21.4 ($NCH_2C_6H_4(CH_3)$-3), 48.9 ($NCH_2C_6H_4(CH_3)$-3), 110.1, 120.2, 122.4, 123.2, 124.2, 127.8, 128.9, 138.9 (NC_6H_4N, $NCH_2C_6H_4(CH_3)$-3), 143.8 (N*C*HN). Calc. for $C_{15}H_{14}N_2$ (222.3): C, 81.05; H, 6.35; N, 12.60. Found: C, 80.90; H, 6.39; N, 12.71%.

$Mn(CO)_3$(bpy)Br (4)

Yield: 580 mg (85%). ^{1}H NMR (500 MHz, DMSO-D_6): δ (ppm) = 7.72 (s, 2H, 5/5'), 8.23 (s, 2H, 4/4'), 8.65 (s, 2H, 3/3'), 9.19 (s, 2H, 6/6'). ^{13}C NMR (500 MHz, DMSO-D_6): δ (ppm) = 123.1 (5/5'), 126.7 (2/2'), 139.1 (4/4'), 153.3 (3/3'), 154.9 (6/6'), 181.3, 186.6, 192.1 (CO). Anal. Calc. for

$C_{13}H_8N_2O_3BrMn$ (375.06): C, 41.63; H, 2.15; N, 7.47. Found: C, 41.57; H, 2.05; N, 7.51%. IR (cm^{-1}, ATR): ν= 1471.8, 1442.3 (s, C-H), 1604.5 (s, C-N), 2019.6, 1938.3, 1912.4 (s, CO).

$[Mn(CO)_3(bpy)\{N\text{-}(3\text{-chlorobenzyl})benzimidazole\}]PF_6$ (5)

Yield: 135.00 mg (69.6%). ^{1}H NMR (300 MHz, DMSO-D_6): δ (ppm)= 5.36 (s, 2H, $NCH_2C_6H_4Cl$), 6.91 (s, 1H, NC*H*N), 8.04 (s, 1H, $NCH_2C_6H_4Cl$), 7.88-7.65 (m, 5H, $NCH_2C_6H_4Cl$, NC_6H_4N), 7.40-7.19 (m, 3H, $NCH_2C_6H_4Cl$, NC_6H_4N), 7.55 (t, J=3.9, 1H, $NCH_2C_6H_4Cl$), 8.31 (d, J=12.3, 2H, $NC_{10}H_8N$), 8.62 (d, J=6.0, 2H, $NC_{10}H_8N$), 9.48 (d, J=3.6, 2H, $NC_{10}H_8N$). ^{13}C NMR (300 MHz, DMSO-D_6): δ (ppm) = 47.16 ($NCH_2C_6H_4Cl$), 137.78 (NCHN), 145.77, 144.38, 140.92, 132.84, 130.54, 127.064, 125.87, 123.30, 117.12, 116.68, 113.42, 112.32 ($NCH_2C_6H_4Cl$, NC_6H_4N), 154.96, 154.63, 140.29, 128.03, 124.00 ($NC_{10}H_8N$). LCMS: m/z 571.034 $[M\text{-bpy}]^+$. IR (cm^{-1}, ATR): ν= 1446.6.7, 1473.6 (s, C-H), 1604.8 (s, C-N), 1925.0, 2033.0 (s, CO).

$[Mn(CO)_3(bpy)\{N\text{-}(3\text{-methoxybenzyl})benzimidazole\}]PF_6$ (6)

Yield: 163.02 mg (84.6%). ^{1}H NMR (300 MHz, DMSO-D_6): δ (ppm)= 3.67 (s, 3H, $NCH_2C_6H_4OCH_3$), 5.30 (s, 2H, $NCH_2C_6H_4OCH_3$), 9.48 (s, 1H, NC*H*N), 9.70-6.43 (m, 16H, $NCH_2C_6H_4OCH_3$, $NC_{10}H_8N$, NC_6H_4N). ^{13}C NMR (300 MHz, DMSO-D_6): δ (ppm) = 48.43 ($NCH_2C_6H_4OCH_3$), 55.55 ($NCH_2C_6H_4OCH_3$), 137.38 (NCHN), 159.82, 155.51, 146.31, 141.87, 139.0, 133.54, 119.70, 117.63, 112.94 ($NCH_2C_6H_4CH_3$, NC_6H_4N), 155.23, 140.88, 130.31, 124.54, 113.78 ($NC_{10}H_8N$). LCMS: m/z 576.15 $[M\text{-PF6}]^+$. IR (cm^{-1}, ATR): ν= 1442.7, 1492.9, 1516.1 (s, C-H), 1604.8 (s, C-N), 2033.0, 1928.8 (s, CO).

$[Mn(CO)_3(bpy)\{N\text{-}(3\text{-methylbenzyl})benzimidazole\}]PF_6$ (7)

Yield: 167.30 mg (88.8%). ^{1}H NMR (300 MHz, DMSO-D_6): δ (ppm)= 2.19 (s, 3H, $NCH_2C_6H_4CH_3$), 9.47 (s, 2H, $NC_{10}H_8N$), 5.30 (s, 2H, $NC_{10}H_8N$), 8.51-6.72 (m, 15H, $NC_{10}H_8N$, $NCH_2C_6H_4CH_3$, NC_6H_4N). ^{13}C NMR (300 MHz, DMSO-D_6): δ (ppm) =20.85 ($NCH_2C_6H_4CH_3$), 47.86 ($NCH_2C_6H_4CH_3$), 136.34 (NCHN), 145.67, 144.84, 141.28, 135.18, 132.88, 128.45, 127.66, 124.54, 124.27, 123.77, 123.02, 117.05 ($NCH_2C_6H_4CH_3$, NC_6H_4N), 154.95, 154.69, 140.30, 137.88, 123.97 ($NC_{10}H_8N$). LCMS: m/z 551.13 $[M\text{-bpy}]^+$. IR (cm^{-1}, ATR): ν= 1442.7, 1516.0 (s, C-H), 1604.8 (s, C-N), 2036.8, 1944.5 (sh) 1928.8, 1925.0 (s, CO).

EXPERIMENTAL and COMPUTATIONAL SECTION

General Remarks:

All chemicals were purchased from Sigma Aldrich and used without further purification. All reactions were carried out under an atmosphere of pure argon by using standard Schlenk and vacuum

techniques. Solvents were freshly distilled after refluxing over metallic sodium or phosphorous pentoxide for 3-4 days. IR spectra were recorded on pure solid samples with a Shimadzu IRAffinity-1 ATR spectrometer. Intensities of stretching vibrations were marked as strong(s), medium (m), weak (w), or shoulder (sh). NMR spectra were recorded on a Bruker Ultra Shield 300 MHz spectrometer. Chemical shifts δ in parts per million indicate a downfield shift relative to tetramethylsilane (TMS) and were referenced relative to the signal of the solvents. Coupling constants J are given in hertz. Individual peaks are marked as singlet (s), doublet (d), triplet (t), or multiplet (m). Absorption spectra were measured using a Shimadzu UV-1800 in quartz cuvettes (d=1 cm). Elemental analysis (C, H, and N) of ligands was carried out using a CHNS-932 (LECO) and liquid chromatography-mass spectrometry (LC-MS) of complexes was carried out on an Agilent 1100 Series. The complexes were precipitated as PF_6 salt by anion exchange procedure.

Synthesis of Ligands (1-3):

Compound 1-3 were prepared by similar methods. Small pieces of lithium (45 mmol, 312 mg) were added slowly to ethylene diamine at 110 ^oC. The solution was allowed to reach room temperature after stirring for 1 hour and n-alkylbenzylchloride (50 mmol) and toluene (40 mL) were added. Precipitated lithium chloride was filtered and the N-(n-alkyl benzyl)ethylene diamine was isolated by distillation from the oily mixture (120 ^oC/0.01 mmHg) after solvents were removed under vacuum. N-(n-alkylbenzyl)ethylenediamine (35 mmol) and N,N-dimethylformamide dimethylacetal (40 mmol) were stirred for 2 hours at 100 ^oC and methanol and dimethyl amine were separated at 120 ^oC by distillation. The last product was isolated from yellow oily residual by distillation under vacuum (124 ^oC/0.01 mmHg).

Synthesis of $Mn(CO)_3(bpy)Br$ (4) :

$Mn(CO)_5Br$ (500 mg, 1.82 mmol) and 2,2'-bipyridyl (312.51 mg, 2.00 mmol) were refluxed in diethyl ether for 3 hours under argon atmosphere. Precipitated orange product was filtered and washed with 10 mL cold diethyl ether.

Synthesis of manganese complexes (5-7):

Compounds 5-7 were prepared by similar methods. $Mn(CO)_3(bpy)Br$ (100 mg, 0.267 mmol) were added into the solution of AgOTf (82.2 mg, 0.320 mmol) in acetone (10 mL). Participated AgBr was filtrated by Celite and the ligand was added after stirring for a day at room temperature. Acetone was evaporated under vacuum and KPF_6/methanol solution was added for anion exchange. Precipitated orange product was filtered and washed with 5 mL cold methanol and 10 mL cold diethyl ether.

Myoglobin Assay:

Horse muscle myoglobin solution which prepared by dissolving in PBS (0.1 M, pH=7.4) was reduced to deoxymyoglobin by addition of sodium dithionite solution in PBS (0.1 M, pH=7.4). Stock solutions of complexes 5-7 that measured CO-releasing properties by myoglobin assay were prepared in DMSO. PBS (0.1 M, pH=7.4), 100 mM sodium dithionite (100 µL), 15 µM metal carbonyl complex and 60 µM myoglobin were combined in a cuvette to give a total volume of 1000 µL. It was degassed by bubbling with argon in each step of the procedure. Final solution was put perpendicularly in front of the UV lamp far from 5 cm and all the spectra were collected by Shimadzu UV 1800 UV-Vis Spectrophotometer. Irradiation was made by 366 nm CAMAG UV Lamp in 1 minute intervals during the initial 20 minute and gone on 5 minutes intervals until no more differences in MbCO concentration. All irradiation experiments were carried out in triplicate. Solutions were freshly prepared for the dark stability and photo-activation experiments. Dark stability spectra were collected automatically for established period of time by spectrometer software.

Antioxidant Activity:

DPPH is a stable free radical. Because of having a single electron, DPPH solution in methanol gives strong absorbance at 517 nm. If DPPH abstracts a hydrogen radical from an external source, the absorption decreases stoichiometrically depending on the number of electrons or hydrogen atoms [63]. An established change in absorbance because of the interaction between DPPH and investigated compound could be evaluated as DPPH radical scavenging capacity. 0.2 mM compound in DMSO was mixed with DPPH solution. The mixtures were shaken and incubated at room temperature for 30 min in dark. The decrease in absorbance of DPPH was measured at 517 nm. Inhibition percent was calculated by comparing the absorbance values of control (DPPH + DMSO) and compounds.

Superoxide dismutase (SOD) activities of the compounds were determined by the method based on the photo-reduction of nitroblue tetrazolium (NBT) of Beauchamp and Fridovich [64]. The reaction mixtures were prepared so as to contain 50 mM phosphate buffer (pH 7.8), 0.1 mM EDTA, 13 mM methionine, 75 µM NBT, 2 µM riboflavin and 0.2 mM of each compound. Riboflavin was added as the last component and the reactions were performed for 10 min by placing the tubes under the fluorescent source (24 W). The reaction in each tube was terminated by removing the tubes from the light source. The photo-reduction of NBT was recorded spectrophotometrically at 560 nm and compared with blank sample which had buffer instead of compound.

Nitric oxide scavenging capacity of the compounds was exhibited by Griess reagent method [65, 66]. 0.2 mM compound was mixed with 5 mM sodium nitroprusside in phosphate buffered saline (pH 7.4) to a final volume of 1 mL. All the mixtures were incubated at 25°C for 150 min. During this period, sodium nitroprusside generates nitric oxide, which interacts with oxygen to produce nitrite ions. Compounds which have nitric oxide scavenging ability leads to reduced nitrite ions

production by competing with oxygen. At the end of this period 0.5 mL of 1X Griess reagent (Modified, Sigma) was added. The absorbance was measured at 540 nm.

In order to exhibit the effect of CO releasing on antioxidative activity, the experiments were performed on compounds which exposed to certain wavelength UV-light (366 nm) for 0, 10 and 20 minutes.

For all scavenging activity assays, % inhibition (I%) values caused by the 0.2 mM of compounds were calculated by using the following equation:

$I\% = [(A_{control} - A_{sample})/ A_{blank}] \times 100$

Electrochemistry:

Cyclic voltammograms (CVs) of the compounds were recorded using a CHI Model 600E Potentiostat with 3-electrode configuration. The working electrode was a glassy carbon electrode (GCE) with a diameter of 3 mm. A Pt wire was used as the counter electrode and a Ag/AgCl electrode was used as the reference electrode. The complex molecules were dissolved in acetonitrile and tetra-n-butylammonium perchlorate (TBAP) was used as the supporting electrolyte. Analytical concentration of the solutions was 4.0 mM for each molecule. All the electrochemical experiments were performed after purging a sufficient amount of pure nitrogen gas to the solutions in order to remove the dissolved oxygen.

Theory/Calculation:

DFT calculations were carried out with ORCA version 2.8 using the BP86 functional with the resolution-of-the-identity (RI) approximation, a def2-TZVP/ def2-TZVP/J basis set, the tightscf and grid4 options, and the COSMO solvation model with water as the solvent for geometry optimizations [51-54].

ACKNOWLEDGEMENTS:

Support of Scientific and Technological Research Council of Turkey (TÜBİTAK, Project No: 112T320) is gratefully acknowledged.

REFERENCES

[1] L. Mond, C. Langer, F. Quincke, J. Chem. Soc. (1890) 749-752.

[2] R. Motterlini, L.E. Otterbein, Nat. Rev. Drug Discov. 9 (2010) 728–743.

[3] B.E. Mann, R. Motterlini, Chem. Commun. (2007) 4197-4208.

[4] R. Alberto, R. Motterlini, Dalton Trans. (2007) 1651-1660.

[5] S.W. Ryter, L.E. Otterbein, BioEssays. 26 (2004) 270–280.

[6] T.R. Johnson, B.E. Mann, J.E. Clark, R. Foresti, C.J. Green, R. Motterlini, Angew. Chem. Int. Ed. 42 (2003) 3722-3729.

[7] T.R. Johnson, B.E. Mann, I.P. Teasdale, H. Adams, R. Foresti, C.J. Green, R. Motterlini, Dalton Trans. (2007) 1500-1508.

[8] R. Motterlini, J.E. Clark, R. Foresti, P. Sarathchandra, B.E. Mann, C.J. Green, Circ. Res. 90 (2002) e17-e24.

[9] S.W. Ryter, L.E. Otterbein, BioEssays. 26 (2004) 270–280.

[10] R. Motterlini, B.E. Mann, R. Foresti, Expert Opin.Invest. Drugs. 14 (2005) 1305–1318.

[11] R. Motterlini, P. Sawle, J. Hammad, S. Bains, R. Alberto, R. Foresti, C. Green, FASEB J. 19 (2005) 284–286.

[12] L. Wu, R. Wang, Pharmacol. Rev. 57 (2005) 585–630.

[13] T.R. Johnson, B.E. Mann, J.E. Clark, R. Foresti, C.J. Green, R. Motterlini, Angew. Chem. Int. Ed. 42 (2003) 3722-3729.

[14] R. Motterlini, B. Haas, R. Foresti, Medical Gas Research, 2 (2012) 28.

[15] D. Babu, R. Motterlini, R.A. Lefebvre, British Journal of Pharmacology, 172 (2015) 1157-1573.

[16] K. Srisook, S.S. Han, H.Y. Choi, M.H. Li, H. Ueda, C. Kim, Y.N. Cha, Biochemical Pharmacology, 71 (2006) 306-318.

[17] O. DeBacker, E. Elinck, B. Blanckaert, L. Leybaert, R. Motterlini, R.A. Lefebvre, Gut, 58 (2009) 347-356.

[18] B.D. Lamon, F.F. Zhang, N. Puri, S.V. Brodsky, M.S. Goligorsky, A. Nasjletti, Circulation Research. 105 (2009) 775-783.

[19] P. Naik, P. Murumkar, R. Giridhar, M.R. Yadav, Bioorg. Med. Chem. 18 (2010) 8418-8456.

[20] M. Sabat, J.C. VanRens, M.J. Laufersweiler, T.A. Brugel, J. Maier, A. Golebiowski, M.J. Janusz, J. Bioorg. Med. Chem. Lett. 16 (2006) 5973-5977.

[21] M. Masaki, T. Yamakawa, Y. Nomura, H. Matsukura, U.S. Patent 5576, 341 (1996).

[22] L. Garuti, M. Roberti, G. Gentilomi, II Farmaco 55 (2000) 35-39.

[23] R.L. Lombardy, F.A. Tanious, K. Ramachandran, R.R. Tidwell and W.D. Wilson, J. Med. Chem. 39 (1996) 1452.

[24] F. Kratz, B. Nuber, J. Weiss, B.K. Keppler, Polyhedron. 11 (1992) 487.

[25] H.M. Refaat, Eur. J. Med. Chem. 45 (2010) 2949-2956.

[26] T.A. Kabanos, A.D. Kersmidas, D. Mentzafos, U. Russo, A.Terzis and J.M. Tsangaris, J. Chem. Soc., Dalton Trans., 2729 (1992).

[27] H. Ueno, S. Katoh, K. Yokota, J.I. Hoshi, M. Hayashi, I. Uchida, K. Aisaka, Y. Hase, H. Cho, Bioorg. Med. Chem. Lett. 14 (2004) 4281-4286.

[28] X. Zhang, M. Urbanski, M. Patel, R.E. Zeck, G.G. Cox, H. Bian, B.R. Conway, M.P. Beavers, P.J. Rybczynski, K.T. Demarest, Bioorg. Med. Chem. Lett. 15 (2005) 5202-5206.

[29] E.R. Cole, G. Crank, A. Salam-Sheikh, J. Agr. Food. Chem. 22 (1974) 918-918.

[30] H.K. Van Dijk, P.C. Servaas, D.J. Stufkens, A. Oskam, Inorg. Chim. Acta. 104 (1998) 179.

[31] R.W. Balk, T.L. Snoeck, D.J. Stufkens, A. Oskam, Inorg. Chem. 19 (1980) 3015.

[32] D.J. Stufkens, *Coord.* Chem. Rev. 104 (1990) 39.

[33] E. Lindsay, A. Jr. Vlcek, C.H. Langford, Inorg. Chem. 32 (1993) 2269.

[34] G.J. Stor, S.L. Morrisson, D.J. Stufkens, A. Oskam, Organometallics. 13 (1994) 2641.

[35] B.D. Rossenaar, E. Lindsay, D.J. Stufkens, A. Jr. Vlcek, Inorg. Chim. Acta 250 (1996) 5.

[36] B.D. Rossenaar, D.J. Stufkens, A. Oskam, J. Fraanje, K. Goubitz, Inorg. Chim. Acta. 247 (1996) 215.

[37] D. Scapens, H. Adams, T.R. Johnson, B.E. Mann, P. Sawle, R. Aqil, T. Perrior, R. Motterlini, Dalton Trans. (2007) 4962-4973.

[38] U. Schatzschneider, Eur. J. Inorg. Chem. (2010) 1451-1467.

[39] U. Schatzschneider, Inorganica Chimica Acta. 374 (2011) 19-23.

[40] I. Chackraborty, S.J. Carrington, P.K. Mascharak, Chem. Med. Chem. 9 (2014) 1266-1274.

[41] G. Dördelmann, T. Meinhardt, T. Sowik, A. Krueger, U. Schatzschneider, Chem. Commun. 48 (2012) 11528-11530.

[42] M.A. Gonzales, P.K. Mascharak, Journal of Inorganic Biochemistry. 133 (2014) 127-135.

[43] P. Govender, S. Pai, U. Schatzschneider, G.S. Smith, Inorg. Chem. 52 (2013) 5470-5478.

[44] N.J. Farrer, L. Salassa, P.J. Sadler, Dalton. Trans. (2009) 10690-10701.

[45] D.M. Manuta, A.J. Lees, Inorg. Chem. 25 (1986) 1354.

[46] J. Vichova, F. Hartl, A. Jr. Vlcek, J. Am. Chem. Soc. 114 (1992) 10903.

[47] P. Datta, A.P. Mukhopadhyay, P. Manna, E.R.T. Tiekink, P.C. Sil, C. Sinha, Journal of Inorganic Biochemistry. 105 (2011) 577-588.

[48] P. Datta, D. Sardar, A.P. Mukhopadhyay, E. Lopez-Torres, C.J. Pastor, C. Sinha, Journal of Organometallic Chemistry. 696 (2011) 488-495.

[49] I.R. Farrell, F. Hartl, S. Zális, M. Wanner, W. Kaim, A. Jr. Vlček, Inorganica Chimica Acta. 318 (2001) 143-151.

[50] M. Landman, R. Pretorius, B.E. Buitendach, P.H. van Rooyen, J. Conradie, Organometallics. 32 (2013) 5491-5503.

[51] F. Neese, J. Biol. Inorg. Chem. 11 (2006) 702-711.

[52] F. Neese, Wiley interdisciplinary Reviews - Computational Molecular Science. 2 (2012) 73-78

[53] A. Schaefer, H. Horn, R. Ahlrichs, J. Chem. Phys. 97 (1992) 2571.

[54] F. Weigend, R. Ahlrichs, Phys. Chem. Chem. Phys. 7 (2005) 3297.

[55] H.M. Berends, P. Kurz, Inorganica Chimica Acta. 380 (2012) 141-147.

[56] W. Huber, R. Linder, J. Niesel, U. Schatzschneider, B. Spingler, P.C. Kunz, Eur. J. Inorg. Chem. (2012) 3140-3146.

[57] F.J. Garcia-Alonso, V. Riera, M.J. Misas, Transition Met. Chem. 10 (1985) 19-21.

[58] R. Ramachandran, P. Viswanathamurthi, Spectrochimica Acta Part A: Molecular and Biomolecular Spectroscopy 103 (2013) 53–61.

[59] E.Y. Choi, S.H. Choe, J.Y. Hyeon, J. Choi, I. Choi, S.J. Kim, European Journal of Pharmacology. 764 (2015) 22–29.

[60] S.A. Moya, R. Pastene, H.L. Bozec, P.J. Baricelli, A.J. Pardey, J. Gimeno, Inorganica Chimica Acta. 312 (2001) 7-14.

[61] D.A. Kurtz, B. Dhakal, R.J. Hulme, G.S. Nichol, G.A.N. Felton, Inorganica Chimica Acta. 427 (2015) 22-26.

[62] P. Datta, C. Sinha, Polyhedron. 26 (2007) 2433-2439.

[63] Y. Harinath, D.H.K. Reddy, B.N. Kumar, C. Apparao, K. Seshaiah, Spectrochimica Acta Part A: Molecular and Biomolecular Spectroscopy. 101 (2013) 264–272

[64] C. Beauchamp, I. Fridovich, Anal. Biochem. Rev. 44 (1971) 276-287.

[65] L.C. Green, D.A. Wagner, J. Glogowski, P.L. Skipper, J.S. Wishnok, S.R. Tannenbaum. Anal. Biochem. 126 (1982) 131–138.

[66] M.S. Kumar, G. Chakraborty, M. Gupta, U.K. Mazumder, Indian J Exp Biol. 44 (2006) 39-44.

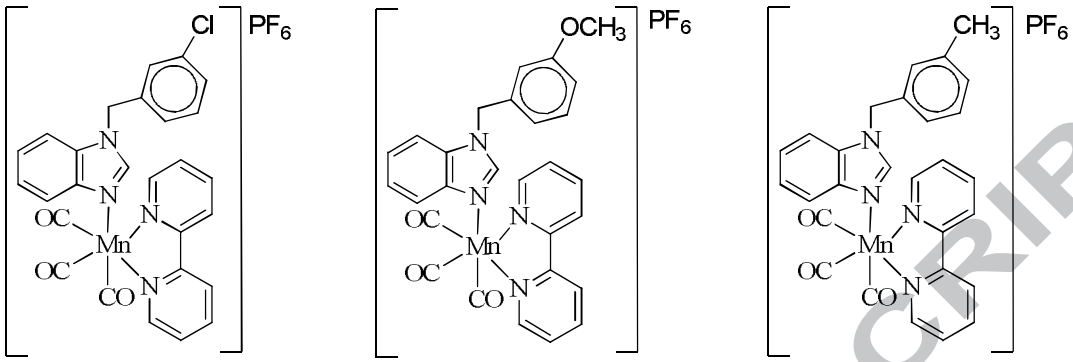

5 **6** **7**

Figure 1. fac-Manganese(I) tricarbonyl bipyridyl complexes with benzimidazole derivatives

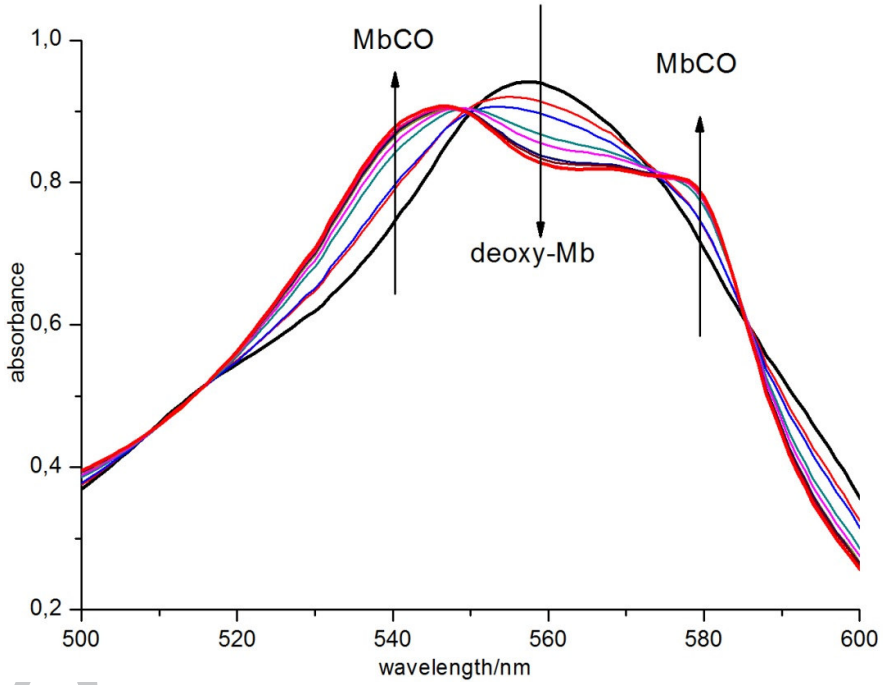

Figure 2. Change of absorption of myoglobin with the irridation at 366 nm UV light for a solution of complex 1 (15 µM) in 0.1 M PBS (pH=7.4) in the presence of myoglobin (60 µM) and sodium dithionite (10 mM) under Argon atmosphere as monitored by UV/Vis spectroscopy

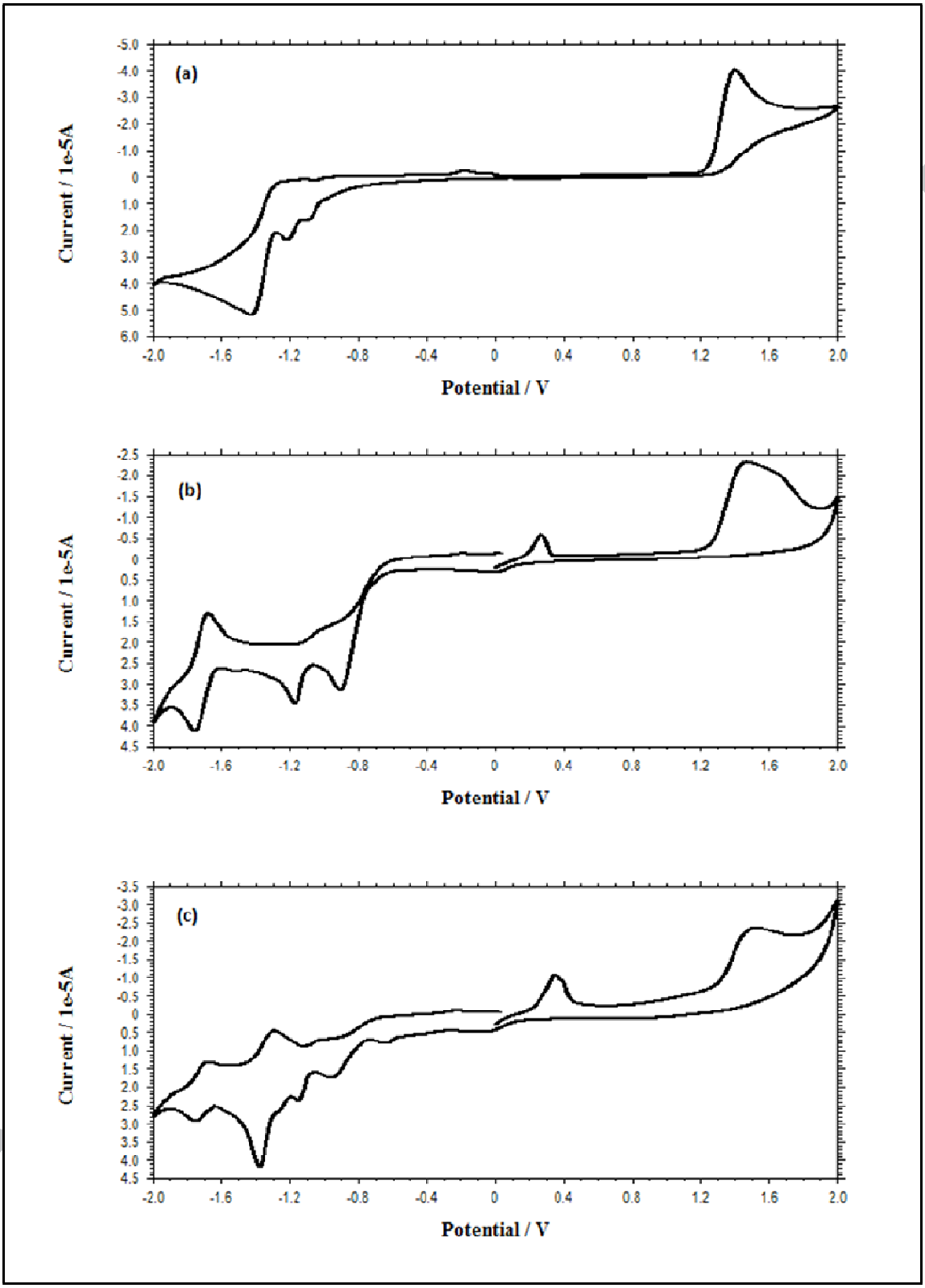

Figure 3. CVs of 4.0 mM solutions of (a) compound **5**, (b) compound **6**, and (c) compound **7** recorded in acetonitrile containing 0.1 M TBAP on GCE. Scan rate = 50 mV s^{-1}

Table 1. CO-Release Data and Absorption Maxima and Extinction Coefficient for Complexes 5-7

Complex	Concentration of MbCO [μM]	Half-life $t_{1/2}$ [min]	Equivalent of CO Released	Percentage CO Released [%]	Wavelength [nm]	ε [$M^{-1}cm^{-1}$]
5	32.84	9.37	2.19	73.0	379	3698.8
6	27.73	11.07	1.85	61.7	378	3465.0
7	29.45	7.31	1.96	65.3	380	2604.2

Table 2. DPPH, SOD and NO radical scavenging ratio as % of 0.2 mM concentrations of some CORMs due to carbon monoxide emissions by exposure to UV light (366 nm) at different time intervals (0, 10 and 20 min)

Complex	DPPH			SOD			NO		
	t=0	t=10	t=20	t=0	t=10	t=20	t=0	t=10	t=20
5	2.25	23.4	20.9	39.2	48.5	51.1	4.96	ND	ND
6	1.53	10.2	5.94	38.3	54.0	60.0	17.0	ND	3.0
7	7.9	14.0	43.9	43.8	61.4	64.2	11.2	ND	ND

ND: Not determined.

Table 3. Energies (in nm), Oscillator Strength (f_{osc}), Main Orbital Contributions, and Type of Transition Involved in the Most Important Singlet Excitations for **5** Calculated with TDDFT/BP86

state	molecular orbitals	main transitions
1	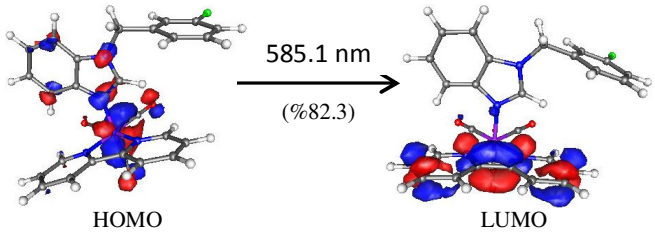	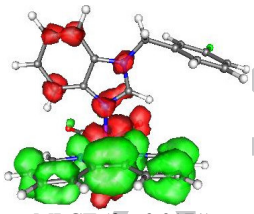
2	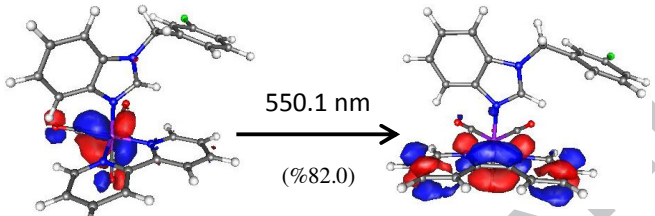	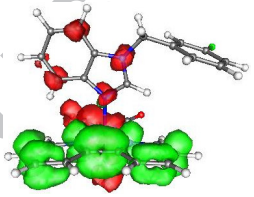
11	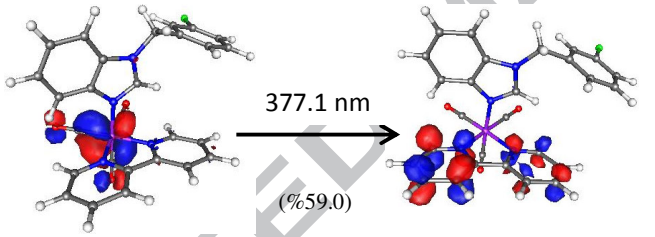	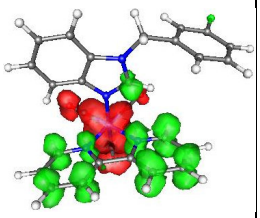
18	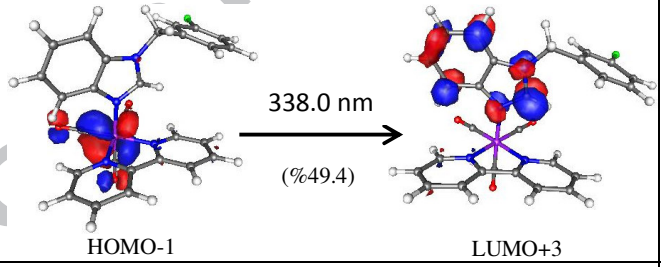	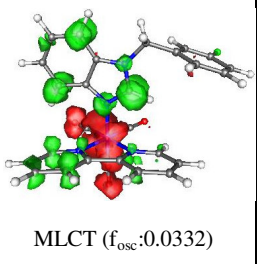
21	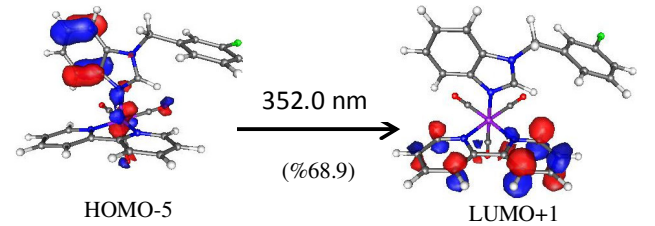	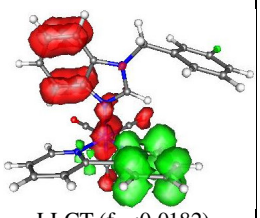

22	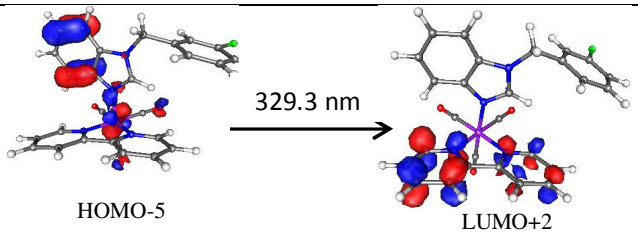	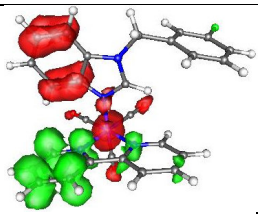	LLCT (f_{osc}:0.0393)
26	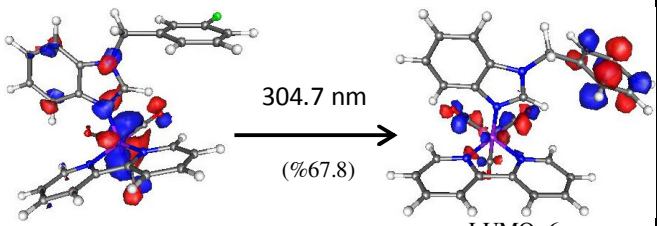	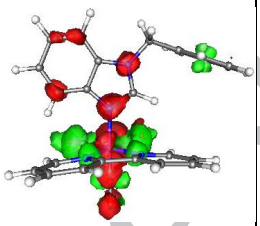	MLCT (f_{osc}:0.0148)
31	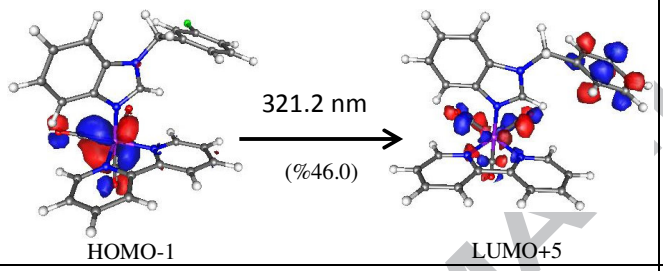	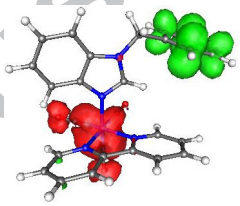	MLCT (f_{osc}:0.0138)
32	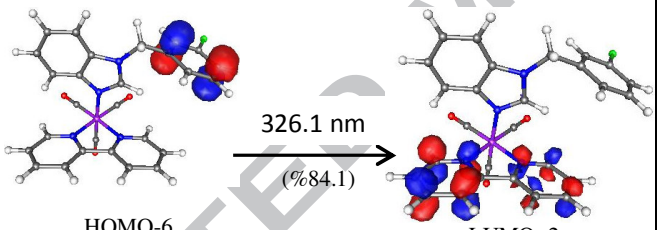	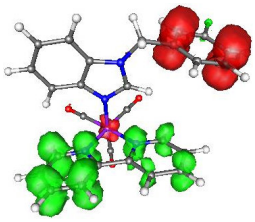	LLCT (f_{osc}:0.0250)

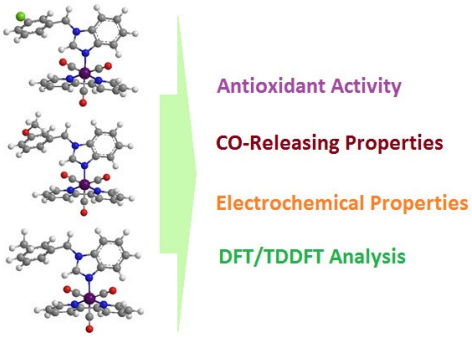

- Synthesis of dark-stable and light-sensitive novel manganese complexes with benzimidazole derivative ligands
- Analytical, spectroscopic and electrochemical characterization of novel benzimidazole substituted manganese complexes
- CO-releasing properties and antioxidant activities of photoCORMs
- DFT/TDDFT analysis of novel manganese complexes with ORCA package program